Available online at www.sciencedirect.com
SCIENCE DIRECT®
Journal of Geochemical Exploration 82 (2004) 79–95
JOURNAL OF GEOCHEMICAL EXPLORATION
www.elsevier.com/locate/jgeoexp

Geochemical exploration in a mountainous area by statistical modeling of polypopulational data distributions

Gerd Rantitsch*

Department of Geosciences, Montanuniversität Leoben, Peter-Tunner-Str. 5, A-8700 Leoben, Austria

Received 20 March 2003; accepted 23 January 2004

Abstract

Variables from a regional geochemical survey are decomposed into parametrical data distribution functions. The results indicate the area and the lithological composition of the catchment basins as factors which control the dispersion of chemical concentrations. From the modeled function parameters, the upper limit of the geochemical background is defined by a 2σ-approximation. The usefulness of this technique is demonstrated in a complex environment (Graz Paleozoic, Eastern Alps).

Keywords: Geochemistry; Stream-sediments; Normal distribution; Lognormal distribution; Graz Paleozoic; Eastern Alps

1. Introduction

Geochemical databases have been created in many European countries by a systematic regional geochemical mapping of overbank and stream sediments (see Darnley, 1995; Bölviken et al., 1996; Plant et al., 2000). The chemical composition of these sediments provides information on weathering and transport processes and on the presence of contaminants and mineral deposits. The complex system, which produces the geochemical data in the sediment, can be reduced to a conceptual model consisting of the components lithology–erosion–transport–accumulation. Consequently, variations in the geochemical signature are related to variations in the lithological composition of the catchment area. As a consequence of this simplification, uncertainty in the database arises from stochasticity in the conceptual model parameters. The data are usually presented as different maps displaying uni- and multivariate geochemical landscapes (dispersion patterns). In this approach, two (among others) problems arise: (1) the relationship between the database and the conceptual model is not represented by these visualizations. Hence, the definition of a threshold between background and anomaly is ambiguous and arbitrary. (2) Interpolation between point data is a fundamental technique of geochemical mapping. In most cases, geostatistics as a ‘‘best linear unbiased estimator’’ is used. However, geostatistical interpolation assumes a homogeneity of the underlying random process. If this approach is applied in a geologically complex area the assumption of homogeneity is not appropriate. Therefore, the application of spatial anomaly detection methods such as moving average techniques, Kriging or fractal modeling are inappropriate.

* Tel.: +43-3842-402-6109; fax: +43-3842-402-6102.
E-mail address: rantit@unileoben.ac.at (G. Rantitsch).

0375-6742/$ - see front matter © 2004 Elsevier B.V. All rights reserved.
doi:10.1016/j.gexplo.2004.01.003

In a geomorphologically and geologically complex setting, an irregular sampling grid (which is unavoidable) produces a geochemical database which is characterized by a strong heterogeneity of the system parameters described above. Consequently, the topographical and lithological characteristics of the catchment basins control the dispersion of chemical concentrations (e.g. Rantitsch, 2000, 2001). The data set is thus characterized by strongly skewed probability distributions which are contaminated with outliers (Reimann and Filzmoser, 2000). If this fact is neglected, the application of (multi- and univariate) statistical and geostatistical techniques will result in biased results.

Reimann and Filzmoser (2000) used the "Geochemical Atlas of the Republic of Austria" (Thalmann et al., 1989) as an example to demonstrate that almost all geochemical and environmental data show neither a normal or a lognormal data distribution. There are several geochemical, geological and analytical processes which result in a complex distribution form of environmental data. Although, this concept is gener-

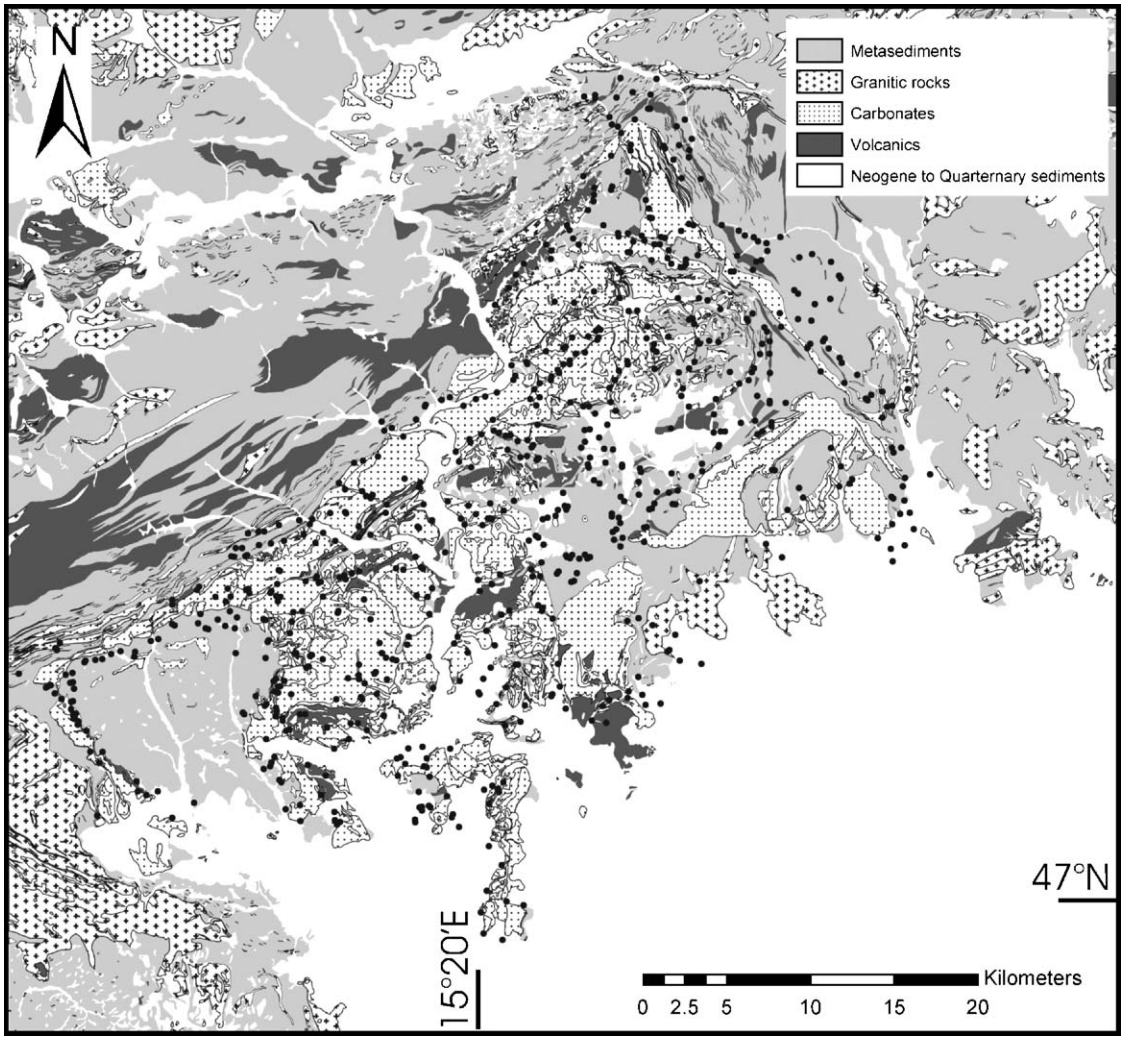

Fig. 1. Geological map of the study area showing the main lithotypes. The Graz Paleozoic is covered by the indicated sample points.

ally accepted, no attempt was undertaken to investigate the nature of this complexity. The main aim of this study is, therefore, to demonstrate that the distribution form of data from a regional geochemical survey (a subset of the "Geochemical Atlas of the Republic of Austria") can be explained by a mixture of parametrical probability density functions. This finding is applied to reconstruct the acting geochemical processes. As an application, the spatial variability of the data is explained by those processes. Geochemical background concentrations depend on the acting geochemical processes and vary therefore in a survey area. They can be interpreted as spatially distributed random variables. Consequently, if the processes are identified, it is possible to define a background concentration based on a user-defined (e.g. Matschullat et al., 2000) method which gives a more realistic view than arbitrary chosen threshold values. The quantification of the background, which visualizes this fact, is the third goal of this study.

Table 1
Elements analyzed, analytical techniques (OES optical spectrometry, XRF wavelength-dispersive X-ray fluorescence spectrometry, Gutzeit semi quantitatively after Gutzeit, ICP-OES induced coupled plasma emission, AAS atomic absorption spectrometry), detection limit (DL), samples below detection in % (%<DL), minimum, maximum, mean, median, mean absolute deviation (MAD), standard deviation (Sdev) of the used data, and *p*-values for a Chi-square (Chi2) Shapiro-Wilk (S-W) and Kolmogorov-Smirnov (K-S) test for normal distribution of the untransformed and transformed (ln-Chi2, ln-S-W, ln-K-S) data

Element	Technique	Unit	DL	%<DL	Min	Max	Mean	Median	MAD	Sdev	Chi2	ln-Chi2	S-W	ln-S-W	K-S	ln-K-S
Ag	OES	ppm	0.02	7.77	0.02	8.1	0.1	0.1	0.1	0.32	0.00	0.00	0.00	0.00	0.00	0.00
Al	XRF	%	0.05	0.00	1.45	15.61	8.9	9.0	4.4	2.55	0.00	0.00	0.01	0.00	0.06	0.00
As	Gutzeit	ppm	2.00	13.96	2	400	12.8	8.0	9.0	25.39	0.00	0.00	0.00	0.00	0.00	0.00
Ba	ICP-OES	ppm	10.00	0.58	10	2190	422.7	390.0	210.0	206.58	0.00	0.00	0.00	0.00	0.00	0.00
Be	ICP-OES	ppm	1.00	7.05	1	11	3.8	4.0	2.0	1.58	0.00	0.00	0.00	0.00	0.00	0.00
Ca	ICP-OES	%	0.01	0.00	0.19	33.03	5.3	3.9	3.1	4.60	0.00	0.00	0.00	0.00	0.00	0.00
Ce	ICP-OES	ppm	10.00	0.00	31	202	95.1	94.0	48.0	24.38	0.00	0.00	0.00	0.00	0.02	0.00
Co	ICP-OES	ppm	3.00	0.00	4	53	17.6	16.0	9.0	8.39	0.00	0.00	0.00	0.00	0.00	0.00
Cr	ICP-OES	ppm	10.00	0.00	11	374	74.1	67.0	38.0	42.07	0.00	0.00	0.00	0.00	0.00	0.00
Cu	ICP-OES	ppm	3.00	0.00	4	105	23.3	23.0	12.0	11.66	0.00	0.00	0.00	0.00	0.00	0.00
Fe	ICP-OES	%	0.01	0.00	0.62	9.21	3.7	3.6	1.8	1.56	0.00	0.00	0.00	0.00	0.01	0.00
Ga	ICP-OES	ppm	3.00	12.23	3	36	17.5	18.0	9.0	9.15	0.00	0.00	0.00	0.00	0.00	0.00
K	XRF	%	0.05	0.00	0.26	4.41	2.3	2.2	1.1	0.69	0.00	0.00	0.00	0.00	0.01	0.00
La	ICP-OES	ppm	10.00	2.59	10	115	44.2	45.0	22.0	16.01	0.00	0.00	0.00	0.00	0.20	0.00
Mg	ICP-OES	%	0.05	0.00	0.3	9.08	1.6	1.4	0.8	1.13	0.00	0.00	0.00	0.00	0.00	0.00
Mn	ICP-OES	%	0.02	0.43	0.015	0.32	0.1	0.1	0.0	0.04	0.00	0.00	0.00	0.00	0.00	0.00
Mo	OES	ppm	0.10	0.00	0.21	3.3	0.9	0.8	0.5	0.42	0.00	0.00	0.00	0.00	0.00	0.00
Na	ICP-OES	%	0.10	2.45	0.1	3.13	0.9	0.8	0.5	0.57	0.00	0.00	0.00	0.00	0.00	0.00
Nb	XRF	ppm	5.00	1.44	5	243	21.9	20.0	10.0	13.73	0.00	0.00	0.00	0.00	0.00	0.00
Ni	ICP-OES	ppm	5.00	0.14	5	134	35.3	34.0	17.0	14.69	0.00	0.00	0.00	0.00	0.00	0.00
P	ICP-OES	%	0.05	2.01	0.05	0.311	0.1	0.1	0.1	0.04	0.00	0.00	0.00	0.01	0.00	0.20
Pb	OES	ppm	3.00	0.00	4	1500	35.8	24.0	18.0	78.50	0.00	0.00	0.00	0.00	0.00	0.00
Rb	XRF	ppm	10.00	0.86	10	219	87.9	83.0	44.0	37.62	0.00	0.00	0.00	0.00	0.00	0.00
Sb	AAS	ppm	2.00	86.76	2	69.4	2.4	2.0	1.1	2.83	0.00	0.00	0.00	0.00	0.00	0.00
Sc	ICP-OES	ppm	1.00	0.00	2	30	12.9	13.0	6.0	5.04	0.00	0.00	0.00	0.00	0.00	0.00
Sn	OES	ppm	1.00	10.36	1	17	3.0	2.9	1.6	1.66	0.00	0.00	0.00	0.00	0.00	0.00
Sr	ICP-OES	ppm	10.00	0.00	36	441	174.1	179.0	90.0	62.97	0.00	0.00	0.00	0.00	0.00	0.00
Th	XRF	ppm	10.00	73.53	10	88	11.9	10.0	6.0	6.14	0.00	0.00	0.00	0.00	0.00	0.00
Ti	ICP-OES	%	0.05	0.00	0.082	2.269	0.6	0.5	0.3	0.35	0.00	0.00	0.00	0.04	0.00	0.20
U	XRF	ppm	5.00	64.60	5	18	5.8	5.0	3.0	1.53	0.00	0.00	0.00	0.00	0.00	0.00
V	ICP-OES	ppm	10.00	0.14	10	325	120.5	119.0	60.0	48.11	0.00	0.00	0.00	0.00	0.00	0.00
W	XRF	ppm	1.00	91.94	1	45	1.3	1.0	1.0	2.25	0.00	0.00	0.00	0.00	0.00	0.00
Y	XRF	ppm	10.00	4.89	10	223	34.0	32.0	17.0	17.01	0.00	0.00	0.00	0.00	0.00	0.00
Zn	ICP-OES	ppm	5.00	0.86	5	4229	94.1	77.0	46.0	176.72	0.00	0.00	0.00	0.00	0.00	0.00
Zr	XRF	ppm	10.00	3.17	10	3587	229.7	221.0	112.0	176.54	0.00	0.00	0.00	0.00	0.00	0.00

2. Database

The study area covers the Graz Paleozoic (Fig. 1), an Austroalpine nappe complex within the Eastern Alps which consists of diverse metasedimentary rocks, carbonates and volcanics, ranging in primary ages from the Silurian up to the Carboniferous. Medium grade metamorphic rocks (gneisses, amphibolites, micaschists, marbles) of the Austroalpine Crystalline Complex underlie tectonically the Graz Paleozoic, whereas Late Cretaceous to Neogene sediments form the overstep sequences.

Multi-element data (695) of the −80 mesh (0.18 mm) of stream-sediments come from the "Geochemical Atlas of the Republic of Austria" (Thalmann et al., 1989). They were analyzed by optical spectrom-

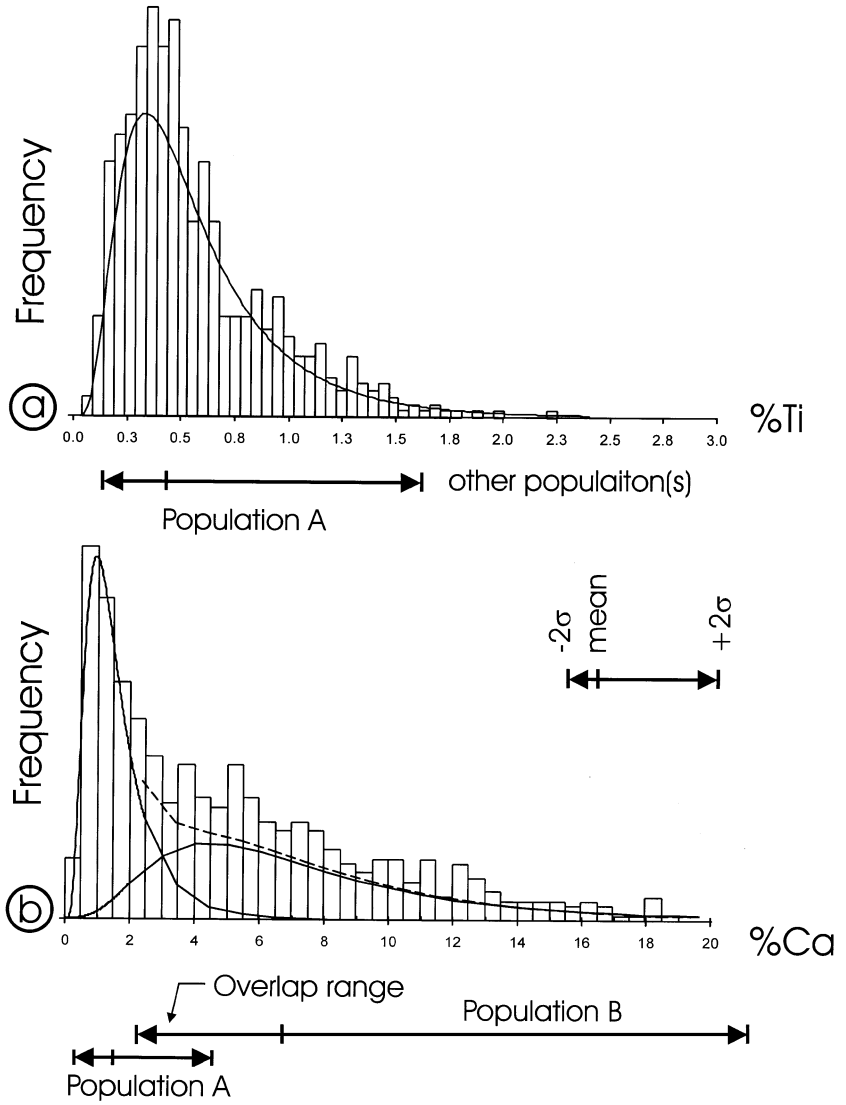

Fig. 2. Histogram and modeled lognormal density trace of Ti (a) and Ca (b). The broken line in (b) is the density trace derived from two overlapping populations. According to a chi-square test, the density traces explain the frequency distribution of the elements. Thresholds for a sample classification are defined by a 2σ-approximation.

etry and induced coupled plasma emission, wavelength-dispersive X-ray fluorescence spectrometry, and atomic absorption spectrometry. In this study, elemental concentrations below the detection limit are set to the value of the detection limit. The element specific analytical procedures and some descriptive statistics of the used data are given in Table 1.

This data set was used by Weber and Davis (1990) to investigate the variation of the elemental concentrations by applying a simultaneous R–Q mode principal component analysis (PCA). Without considering the distribution form of the data, they were able to identify the lithological and mineralogical composition of the catchments and the presence of As, Pb–Zn, and W mineralisations as the main factors which control the spatial structure of this data set.

3. Data processing

In a topographic map of the study area (at a scale of 1:25,000), the hydrological catchment area was digitized manually for each sample location (see Fig. 1). This area is taken as the zone of influence of the sample. A compiled geological map at a scale of 1:50,000 (Fig. 1) was used to evaluate the spatial association between bedrock lithology and stream-sediment geochemistry. This was done by a spatial overlay of the geological map, which was reclassified into five lithotypes (metasediments, granitic rocks, carbonates, volcanics and Neogene to Quaternary sediments), representative for the internal lithological variation, with a map of the catchment areas, using a Geographical Information System. The definition of the lithotypes is based on the likelihood of having similar erodibility.

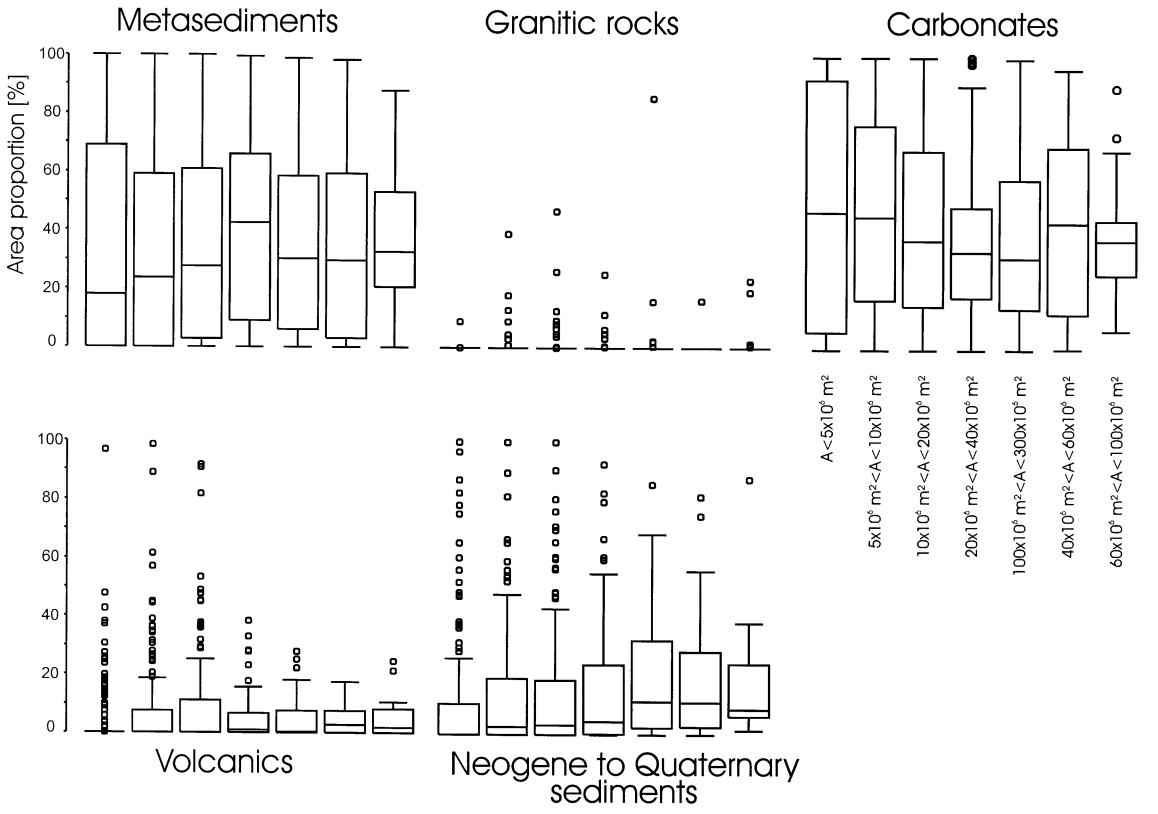

Fig. 3. Lithological composition (in area percentages) of catchment basins with different areas (A). The box plots show the median, the quartiles and the outlier (dots) which are defined by a deviation of more than 1.5 interquartile ranges from the box boundaries.

The goal of the presented approach is the decomposition of the probability functions in components which can be described by a normal or a lognormal function. If a goodness-of-fit test confirms the statistically significant derivation of the observed data from a parametrical probability function, it is assumed that this function is an outcome of the process which controls the spatial pattern of the geochemical landscape. In this study, the chi-square test is used to decide about the rejection of the null hypothesis of normal distribution at a significance level α of 0.05. Because of the high amount of measurements below the detection limit, modeling was prevented for the elements Sb, W, U and Th (Table 1).

In a first experiment, the observed probability distributions are fitted by normal and lognormal distribution functions. To standardize the classification procedure, sample values which deviate with more than two standard deviations from the respective arithmetic or lognormal (Limpert et al., 2001) mean value are interpreted to derive from a different population (Fig. 2). Thus, a 2.3% probability of a rejection error (in the case of two overlapping populations A and B, a sample with a population A value is rejected as population A sample) is accepted. The value of the acceptance error (a population B sample is accepted as population A sample) depends on the characteristics of the overlapping population and the degree of overlap (see Fig. 2). If the null hypothesis cannot be accepted, the second step is the decomposition of the observed distributions in their components (Sinclair, 1974, 1991) by using the software "Tripod®" (Geoecosse, Alloa, Scotland), which is based on a nonlinear least-square decomposition of mixtures of distributions (Clark, 1977). If a polymodal distribution can be modeled by this approach (Fig. 2b) it is assumed that the specific element is influenced by more than one process or source.

The geochemical composition of alluvial sediments which are partly exposed as stream-sediments is a result of denudation within the corresponding catchment basin and is usually related to erosion of the bedrock lithology. If a point source anomaly is present the elemental concentrations are diluted in the downstream direction (Hawkes, 1976). Therefore, secondly it is attempted to achieve a decomposition by a correction of the dilution effect. This is done simply by assessing the elemental concentrations after a classification of the catchments based on the area of the catchment basins. Seven groups are distinguished: group 1 with an area $<5\times10^6$ m^2 ($N=161$), group 2 with an area between 5×10^6 and 10×10^6 m^2 ($N=195$), group 3 with an area between 10×10^6 and 20×10^6 m^2 ($N=161$), group 4 with an area between 20×10^6 and 40×10^6 m^2 ($N=87$), group 5 with an area between 40×10^6 and 60×10^6 m^2

Table 2
Population (Dist norm normal distribution, log lognormal distribution) parameters (perc population percentage of bimodal distributions, arithmetic and logarithmic mean, sdv arithmetic and logarithmic standard deviation) and Chi-square statistic (Chi2), degrees of freedom (*df*) and *p*-values for a Chi-square (Chi2) test for normal distribution

Element	Dist	perc	Mean	sdv	Chi2	*df*	*p*	Min	Mean	Max
Al	norm		8.96	2.61	58.41	51	0.22	3.73	8.96	14.18
Ca	log	41	0.30	0.60	58.50	49	0.17	0.40	1.34	4.50
	log	59	1.91	0.57				2.16	6.74	21.01
Cr	log	46	3.75	0.41	53.53	46	0.21	18.77	42.67	97.05
	log	54	4.41	0.27				48.05	82.48	141.60
Fe	log	41	0.83	0.45	54.29	49	0.28	0.94	2.29	5.61
	log	59	1.48	0.28				2.49	4.38	7.72
K	norm		2.18	0.59	61.11	49	0.11	1.00	2.18	3.37
Mg	log		0.28	0.48	68.28	51	0.05	0.50	1.32	3.48
P	log		−2.30	0.33	62.21	46	0.06	0.05	0.10	0.20
Rb	norm	25	58.33	16.58	48.07	48	0.47	25.16	58.33	91.50
	norm	75	97.58	37.04				23.50	97.58	171.65
Ti	log		−0.73	0.61	56.48	54	0.38	0.14	0.48	1.64

Minimum (min) and maximum (max) values of the populations are calculated by a distance of more than two standard deviations from the arithmetic or lognormal mean value (mean). Elements, which cannot be described by parametrical distribution functions, are not included.

Table 3
Population (Dist norm normal distribution, log lognormal distribution) parameters (perc population percentage of bimodal distributions, arithmetic and logarithmic mean, sdv arithmetic and logarithmic standard deviation) and Chi-square statistic (Chi2), degrees of freedom (*df*) and *p*-values for a Chi-square (Chi2) test for normal distribution in seven groups of different catchment areas (AG 1 with an area $<5 \times 10^6$ m^2, $N=161$, AG 2 with an area between 5×10^6 and 10×10^6 m^2, $N=195$, AG 3 with an area between 10×10^6 and 20×10^6 m^2, $N=161$, AG 4 with an area between 20×10^6 and 40×10^6 m^2, $N=87$, AG 5 with an area between 40×10^6 and 60×10^6 m^2, $N=38$, AG 6 with an area between 60×10^6 and 100×10^6 m^2, $N=32$ and AG 7 with an area>100×10^6 m^2, $N=21$)

Element	Dist	AG	perc	Mean	sdv	Chi2	*df*	*p*	Min	Mean	Max
Ag	log	1		−2.51	0.58	11.28	8	0.19	0.03	0.08	0.26
	log	2		−2.54	0.71	27.22	17	0.06	0.02	0.08	0.32
		3									
	log	4	48	−2.61	0.69	5.86	2	0.06	0.02	0.07	0.29
			52	−2.31	0.25				0.06	0.10	0.16
		5		−2.41	0.57	2.61	3	0.40	0.03	0.09	0.28
	log	6		−2.25	0.37	0.60	2	0.75	0.05	0.11	0.22
	log	7		−2.16	0.42	0.76	1	0.40	0.05	0.12	0.27
Al	norm	1		8.54	2.62	11.45	10	0.40	3.29	8.54	13.79
	norm	2		8.80	2.64	16.23	13	0.25	3.52	8.80	14.08
	norm	3		9.01	2.56	8.44	11	0.65	3.88	9.01	14.13
	norm	4		9.31	2.47	13.22	7	0.07	4.36	9.31	14.26
	norm	5		8.92	2.21	2.50	3	0.40	4.50	8.92	13.34
	norm	6		9.92	3.10	1.79	3	0.60	3.71	9.92	16.12
	norm	7		10.23	0.85	1.38	1	0.25	8.53	10.23	11.93
As	log	1		2.44	0.67	7.83	4	0.10	2.99	11.45	43.79
	log	2		2.43	1.00	0.59	3	0.90	1.53	11.35	84.34
	log	3		2.41	0.78	10.38	5	0.07	2.34	11.10	52.68
	log	4		2.30	0.59	6.65	4	0.15	3.05	9.94	32.39
	log	5		2.33	0.60	3.78	2	0.15	3.07	10.29	34.45
	log	6		2.34	0.92	0.35	2	0.85	1.64	10.38	65.70
	log	7		2.35	0.10	4.67	3	0.20	8.54	10.49	12.88
Ca	log	1		1.20	1.08	17.28	10	0.07	0.38	3.32	28.89
	log	2	40	0.52	0.79	6.96	9	0.60	0.34	1.68	8.19
			60	1.97	0.55				2.39	7.15	21.45
	log	3	41	0.28	0.65	4.81	6	0.60	0.36	1.32	4.89
			59	1.95	0.51				2.54	7.00	19.29
	log	4	44	0.29	0.43	0.18	2	0.92	0.56	1.33	3.15
			56	1.82	0.43				2.60	6.15	14.59
	log	5	24	−0.09	0.29	0.22	1	0.60	0.51	0.92	1.65
			76	1.64	0.69				1.30	5.18	20.68
	log	6		1.08	1.46	4.76	2	0.07	0.16	2.94	55.00
	log	7		0.90	1.26	0.85	1	0.40	0.20	2.47	30.74
Ba	norm	1		406.98	188.58	10.85	10	0.40	29.82	406.98	784.13
	norm	2		446.79	178.53	2.04	5	0.85	89.73	446.79	803.85
	log	3		5.97	0.33	10.66	8	0.40	203.28	392.52	757.94
	norm	4		438.40	165.69	10.31	6	0.12	107.02	438.40	769.78
	norm	5		357.18	104.80	1.32	2	0.65	147.58	357.18	566.77
	norm	6		389.71	160.46	5.06	3	0.40	68.78	389.71	710.63
	log	7		5.98	0.61	2.04	1	0.15	116.15	393.66	1334.22
Be	norm	1		3.16	1.57	3.42	2	0.18	0.02	3.16	6.31
	norm	2		3.64	1.24	0.97	2	0.60	1.17	3.64	6.12
	norm	3		3.65	1.49	2.26	4	0.65	0.67	3.65	6.64
	norm	4		3.43	1.57	1.63	1	0.20	0.28	3.43	6.58
	norm	5		3.43	1.57	1.63	1	0.20	0.28	3.43	6.58
	norm	6		3.90	1.78	2.03	2	0.40	0.34	3.90	7.46
	norm	7		4.24	1.89	1.58	1	0.20	0.45	4.24	8.03

(continued on next page)

Table 3 (*continued*)

Element	Dist	AG	perc	Mean	sdv	Chi2	*df*	*p*	Min	Mean	Max
Ce	norm	1		90.33	27.86	17.08	10	0.08	34.60	90.33	146.06
	log	2		4.60	0.27	3.38	6	0.75	57.75	99.31	170.75
	norm	3		95.37	23.28	11.13	10	0.35	48.80	95.37	141.93
	norm	4		96.76	22.15	3.87	6	0.70	52.46	96.76	141.06
	norm	5		90.15	18.47	6.94	4	0.15	53.20	90.15	127.10
	norm	6		98.47	23.48	1.57	3	0.60	51.52	98.47	145.43
	norm	7		86.41	24.97	0.42	1	0.85	36.46	86.41	136.35
Co	log	1		2.70	0.57	12.12	10	0.28	4.75	14.89	46.69
	log	2		2.79	0.48	7.32	11	0.75	6.27	16.32	42.45
	log	3		2.78	0.48	19.45	11	0.07	6.17	16.20	42.53
	log	4		2.84	0.37	6.12	4	0.40	8.25	17.15	35.66
	log	5		2.70	0.46	2.66	4	0.60	5.93	14.95	37.72
	log	6		2.87	0.56	1.16	3	0.75	5.74	17.58	53.88
	log	7		2.73	0.52	0.49	1	0.45	5.45	15.34	43.15
Cr	log	1	43	3.57	0.33	1.94	4	0.75	18.42	35.64	68.94
			57	4.38	0.23				50.56	79.55	125.16
	log	2		4.16	0.52	16.29	11	0.15	22.51	63.85	181.13
	log	3		4.23	0.53	9.42	9	0.40	23.93	68.48	195.96
	log	4	43	4.08	0.56	0.41	2	0.80	19.38	58.94	179.25
			57	4.33	0.25				45.81	75.99	126.04
	log	5		4.10	0.44	3.46	4	0.45	25.06	60.24	144.79
	log	6		4.20	0.49	1.89	3	0.60	24.98	66.85	178.95
	log	7		4.14	0.59	2.64	1	0.08	19.26	62.95	205.76
Cu	log	1	25	2.17	0.33	9.60	6	0.40	4.55	8.74	16.80
			75	3.24	0.39				11.74	25.56	55.65
	log	2	46	2.53	0.38	13.79	8	0.08	5.86	12.60	27.12
			54	3.35	0.27				16.72	28.62	48.97
	log	3		3.10	0.50	14.05	10	0.15	8.12	22.20	60.69
	log	4		3.14	0.49	9.82	5	0.07	8.60	23.04	61.70
	log	5		3.00	0.56	4.31	4	0.40	6.49	20.00	61.59
	log	6		3.10	0.68	5.02	2	0.15	5.71	22.15	85.99
	log	7		3.01	0.53	0.96	1	0.30	6.97	20.29	59.02
Fe	log	1	28	0.47	0.24	3.63	5	0.30	1.00	1.61	2.59
			72	1.43	0.31				2.23	4.17	7.79
	log	2	30	0.78	0.15	7.72	6	0.40	1.60	2.17	2.95
			70	1.48	0.26				2.61	4.37	7.31
	norm	3		3.76	1.58	16.65	10	0.08	0.60	3.76	6.91
	norm	4		3.81	1.42	8.66	6	0.15	0.98	3.81	6.65
	norm	5		3.53	1.41	2.57	4	0.60	0.70	3.53	6.36
	norm	6		3.65	1.60	5.09	3	0.15	0.45	3.65	6.84
	norm	7		3.51	1.85	0.17	1	0.70	−0.18	3.51	7.20
Ga	log	1	76	2.79	0.40	5.01	4	0.25	7.36	16.30	36.12
			24	3.32	0.04				25.57	27.58	29.74
		2									
	log	3		3.03	0.38	8.36	5	0.15	9.78	20.80	44.24
	norm	4	66	2.83	0.34	1.33	2	0.55	8.61	17.01	33.60
			34	3.36	0.07				24.80	28.75	33.34
	log	5		3.05	0.37	0.14	1	0.70	9.95	21.06	44.56
	log	6		3.21	0.33	0.82	1	0.40	12.89	24.77	47.59
	norm	7		22.48	4.94	3.57	2	0.15	12.59	22.48	32.37
K	norm	1		2.22	0.61	14.80	9	0.10	1.01	2.22	3.43
	norm	2		2.33	0.73	11.71	12	0.45	0.87	2.33	3.79
	norm	3		2.18	0.70	14.17	9	0.15	0.78	2.18	3.58
	norm	4		2.29	0.64	0.84	5	0.96	1.01	2.29	3.58

Table 3 (*continued*)

Element	Dist	AG	perc	Mean	sdv	Chi2	*df*	*p*	Min	Mean	Max
K	norm	5		2.15	0.58	1.27	3	0.75	0.98	2.15	3.32
	norm	6		2.14	0.47	4.90	3	0.30	1.19	2.14	3.08
	norm	7		2.22	0.40	0.23	1	0.60	1.43	2.22	3.01
La	norm	1		41.79	17.39	29.16	24	0.25	7.01	41.79	76.57
	norm	2		45.00	15.57	15.60	12	0.25	13.86	45.00	76.15
	norm	3		44.54	16.21	7.43	10	0.65	12.11	44.54	76.96
	norm	4		45.86	12.06	15.36	14	0.40	21.74	45.86	69.98
	norm	5		40.84	11.50	2.40	3	0.50	17.84	40.84	63.84
	norm	6		43.29	17.42	2.38	3	0.50	8.44	43.29	78.14
	norm	7		39.88	15.08	0.87	1	0.40	9.72	39.88	70.05
Mg	log	1		0.26	0.54	3.87	8	0.85	0.44	1.29	3.79
	log	2		0.35	0.51	13.81	12	0.35	0.52	1.43	3.92
	log	3		0.34	0.55	3.97	9	0.92	0.47	1.41	4.22
	log	4		0.32	0.43	4.38	5	0.50	0.59	1.38	3.22
	log	5		0.20	0.45	4.35	3	0.40	0.50	1.23	2.99
	log	6		0.31	0.36	1.14	3	0.75	0.67	1.37	2.78
	log	7		0.02	0.49	2.60	2	0.25	0.38	1.02	2.72
Mn	log	1	36	− 3.21	0.36	1.47	5	0.92	0.02	0.04	0.08
			64	− 2.18	0.28				0.06	0.11	0.20
	log	2	25	− 3.31	0.29	8.14	9	0.55	0.02	0.04	0.07
			75	− 2.33	0.36				0.05	0.10	0.20
	norm	3		0.09	0.04	14.66	8	0.07	0.01	0.09	0.16
	norm	4		0.09	0.04	6.54	5	0.25	0.01	0.09	0.17
	norm	5		0.09	0.04	5.90	4	0.25	0.01	0.09	0.17
	norm	6		0.10	0.04	0.39	3	0.93	0.01	0.10	0.19
	norm	7		0.09	0.03	0.51	1	0.55	0.02	0.09	0.15
Mo	log	1		− 0.20	0.42	16.98	10	0.08	0.36	0.82	1.89
	log	2		− 0.18	0.43	11.16	12	0.55	0.36	0.84	1.97
	log	3		− 0.17	0.36	11.49	8	0.25	0.42	0.85	1.73
	log	4		− 0.16	0.37	7.77	5	0.15	0.41	0.85	1.77
	log	5		− 0.26	0.41	2.16	4	0.70	0.34	0.77	1.73
	log	6		− 0.10	0.32	5.53	3	0.15	0.48	0.91	1.72
	log	7		− 0.27	0.32	2.26	1	0.15	0.40	0.77	1.45
Na	log	1		− 0.21	0.62	13.05	8	0.15	0.24	0.81	2.82
	log	2		− 0.13	0.55	5.44	11	0.92	0.30	0.88	2.64
	log	3		− 0.07	0.55	3.36	8	0.92	0.31	0.93	2.81
	log	4		− 0.13	0.54	2.11	6	0.92	0.30	0.88	2.58
	log	5		− 0.27	0.62	9.00	4	0.07	0.22	0.77	2.64
	log	6		− 0.06	0.51	0.91	1	0.40	0.34	0.94	2.62
	norm	7		0.94	0.61	5.25	2	0.08	− 0.28	0.94	2.16
Nb	log	1	74	2.80	0.34	1.64	3	0.60	8.34	16.42	32.32
			26	3.45	0.14				23.97	31.46	41.29
	log	2		3.06	0.43	16.71	10	0.07	8.97	21.25	50.33
	log	3		3.07	0.44	7.42	8	0.45	8.89	21.62	52.56
	log	4		2.96	0.50	0.50	4	0.97	7.04	19.22	52.43
	log	5		3.18	0.36	0.64	3	0.85	11.61	23.98	49.56
	log	6		2.93	0.49	3.54	2	0.15	7.09	18.73	49.48
	log	7		2.85	0.45	1.60	1	0.20	6.99	17.32	42.90
Ni	norm	1		33.54	14.08	14.71	9	0.10	5.39	33.54	61.69
	norm	2		33.90	11.82	20.63	12	0.07	10.26	33.90	57.54
	log	3		3.52	0.42	5.54	9	0.75	14.60	33.85	78.48
	log	4		3.54	0.34	3.24	5	0.60	17.50	34.47	67.90
	log	5		3.41	0.37	4.16	4	0.40	14.31	30.21	63.78

(continued on next page)

Table 3 (*continued*)

Element	Dist	AG	perc	Mean	sdv	Chi2	*df*	*p*	Min	Mean	Max
Ni	log	6		3.55	0.42	1.56	2	0.40	14.99	34.97	81.57
	log	7		3.43	0.39	0.46	1	0.50	14.18	30.86	67.20
P	log	1		− 2.33	0.38	10.01	9	0.40	0.05	0.10	0.21
	log	2		− 2.29	0.30	10.08	12	0.60	0.06	0.10	0.19
	log	3		− 2.27	0.33	9.29	8	0.40	0.05	0.10	0.20
	log	4		− 2.25	0.33	3.18	6	0.75	0.05	0.11	0.20
	log	5		− 2.35	0.40	7.45	3	0.08	0.04	0.10	0.21
	log	6		− 2.24	0.37	2.64	2	0.25	0.05	0.11	0.22
	log	7		− 2.35	0.38	0.99	1	0.30	0.04	0.09	0.20
Pb	log	1		3.14	0.50	5.32	8	0.75	8.43	23.07	63.13
	log	2		3.12	0.50	15.01	11	0.15	8.31	22.64	61.68
	log	3		3.25	0.49	11.09	9	0.25	9.71	25.69	67.97
	log	4		3.28	0.44	6.58	5	0.40	11.01	26.45	63.56
	log	5		3.21	0.45	3.77	3	0.25	10.05	24.86	61.50
	log	6		3.33	0.55	1.47	2	0.40	9.19	27.80	84.07
	log	7		3.35	0.44	1.79	1	0.15	11.78	28.50	68.95
Rb	log	1	49	3.94	0.26	5.45	5	0.40	30.88	51.56	86.09
			51	4.70	0.26				65.62	109.72	183.44
	log	2		4.46	0.46	18.24	13	0.15	34.59	86.10	214.33
	log	3		3.27	0.50	14.45	8	0.08	9.66	26.19	70.96
	log	4	7	2.79	0.28	3.11	1	0.08	9.30	16.24	28.37
			93	4.47	0.36				42.49	87.03	178.25
	log	5		4.43	0.33	1.54	3	0.55	43.36	83.55	161.02
	log	6		4.39	0.28	1.97	3	0.60	46.09	80.27	139.80
	log	7		4.50	0.25	1.62	1	0.20	54.24	90.08	149.59
Sn	log	1		1.22	0.27	5.36	4	0.25	1.98	3.40	5.84
	log	2		1.37	0.31	2.90	4	0.60	2.14	3.95	7.27
		3									
	log	4		1.21	0.29	3.98	5	0.60	1.89	3.35	5.96
	log	5		1.16	0.41	2.37	2	0.30	1.41	3.20	7.26
	log	6		1.16	0.57	1.49	2	0.40	1.01	3.17	9.98
	log	7		1.21	0.33	0.33	1	0.75	1.73	3.35	6.50
Sr	norm	1		156.79	58.95	16.06	10	0.10	38.89	156.79	274.70
	norm	2		168.73	58.33	42.59	31	0.08	52.06	168.73	285.40
	norm	3		176.36	59.31	18.81	28	0.93	57.74	176.36	294.98
		4									
	norm	5		170.84	56.42	4.16	3	0.25	58.00	170.84	283.69
	norm	6		173.65	39.89	6.85	3	0.08	93.87	173.65	253.42
	norm	7		174.35	67.59	2.31	1	0.15	39.17	174.35	309.54
Ti	log	1		− 0.76	0.64	13.89	11	0.25	0.13	0.47	1.68
	log	2		− 0.76	0.61	6.06	13	0.93	0.14	0.47	1.58
	log	3		− 0.73	0.60	10.57	10	0.40	0.15	0.48	1.61
	log	4		− 0.64	0.55	7.19	6	0.30	0.18	0.53	1.56
	log	5		− 0.70	0.51	0.71	4	0.95	0.18	0.49	1.38
	log	6		− 0.52	0.81	4.17	2	0.15	0.12	0.59	2.98
		7									
Zn	log	1		4.39	0.34	3.13	7	0.85	40.61	80.96	161.37
	log	2		4.39	0.37	12.78	10	0.25	38.63	80.94	169.58
	log	3		4.37	0.47	10.16	8	0.25	30.68	78.89	202.84
	log	4		4.34	0.42	4.55	5	0.40	33.12	76.40	176.23
	log	5		4.28	0.44	9.10	5	0.15	29.95	72.32	174.64
	log	6		4.42	0.35	0.84	3	0.85	41.62	83.22	166.42
	log	7		4.16	0.44	0.28	1	0.60	26.38	63.99	155.24
Y	log	1		3.50	0.40	0.99	5	0.97	15.00	33.25	73.71
		2									

Table 3 (*continued*)

Element	Dist	AG	perc	Mean	sdv	Chi2	*df*	*p*	Min	Mean	Max
Y	log	3		3.51	0.35	6.60	7	0.40	16.70	33.46	67.04
	log	4		3.58	0.41	0.75	4	0.93	15.91	35.97	81.32
	log	5		3.35	0.45	3.13	4	0.60	11.73	28.60	69.75
	log	6		3.61	0.19	4.23	2	0.15	25.32	36.95	53.94
		7									
V	log	1		4.72	0.42	12.23	10	0.40	48.18	112.60	263.12
	norm	2		119.63	42.19	9.67	11	0.60	35.24	119.63	204.02
	norm	3		122.84	48.75	11.25	10	0.30	25.35	122.84	220.33
	norm	4		123.95	49.14	7.56	5	0.15	25.68	123.95	222.23
	norm	5		107.58	48.22	4.91	4	0.30	11.14	107.58	204.02
	norm	6		120.98	52.98	1.52	2	0.40	15.01	120.98	226.95
	norm	7		121.00	53.02	3.15	1	0.08	14.96	121.00	227.04

Minimum (min) and maximum (max) values of the populations are calculated by a distance of more than two standard deviations from the arithmetic or lognormal mean value (mean). Elements, which cannot be described by parametrical distribution functions, are not included.

($N=38$), group 6 with an area between 60×10^6 and 100×10^6 m^2 ($N=32$) and group 7 with an area $>100 \times 10^6$ m^2 ($N=21$).

In a third experiment, catchment basins which are dominated by a specific lithotype (area percentage of more than 70%) are selected from the database. The distribution functions of the elements in these catchments are analyzed as described above. In this experiment, the area of the catchments is not considered as a modeling parameter.

4. Results

Table 1 shows deviations between mean and median and standard deviation and mean absolute deviation for almost all elements. According to statistical tests, none of the elements follow a normal distribution (Table 1). Furthermore, it can be demonstrated that ln-transformed values do not exhibit a normal distribution (Table 1). An inspection of the box plots in Fig. 3 demonstrates that the lithological composition of the catchments in the seven catchment groups is different. Although the area proportions of metasediments and carbonates is the same in all groups, all other lithotypes are present in varying proportions (Fig. 3).

The probability distributions of the elements Al, K, Mg, P and Ti can be fitted by one single parametrical distribution function. If two overlapping functions are assumed, a statistically significant fit is achieved for the elements Ca, Cr, Fe, Rb (Table 2).

A pooling of the data in seven groups of different catchment areas allows the detection of normal distributions for all groups of the elements Be and La (Table 3). The elements As, Co, Pb and Zn can be described by a normal distribution when they are ln-transformed (Table 3). Some elements (Ba, Ce, Na, Ni, V) show normal and lognormal distribution forms in the different catchment groups (Table 3). Ag, Cu, Mn and Nb are characterized by a bimodal distribution in at least one catchment group (Table 3). The elements Ga, Sr and Y cannot be described completely (Table 3).

Almost all elements can be fitted to parametrical functions if the modeling is restricted to catchments which are dominated by carbonates or metasediments (Table 4). The other lithotypes do not contribute with more than 50% to the lithological composition of the catchments. Therefore, they are combined to a lithological group which is not dominated by carbonates and metasediments. Modeling of this group demonstrates that an inhomogeneous data set cannot be represented completely by parametrical functions for all elements.

5. Discussion

It has been suggested (Reimann and Filzmoser, 2000; Reimann et al., 2002) that geochemical data cannot be represented by parametrical distribution functions. However, in Tables 2–4 it is shown that a parametrical representation can be achieved if the

Table 4
Population (Dist norm normal distribution, log lognormal distribution) parameters (perc population percentage of bimodal distributions, arithmetic and logarithmic mean, sdv arithmetic and logarithmic standard deviation) and Chi-square statistic (Chi2), degrees of freedom (*df*) and *p*-values for a Chi-square (Chi2) test for normal distribution in catchments which are dominated by metasediments, carbonates and all other lithotypes

Element	Dist	%	Mean	sdv	Chi2	*df*	*p*	Min	Mean	Max
Metasediments										
Ag	log		−2.38	0.51	9.74	7	0.20	0.03	0.09	0.26
Al	norm		10.38	2.39	27.54	22	0.15	5.61	10.38	15.15
As	log		2.41	0.57	6.01	5	0.30	3.57	11.12	34.61
Ba	norm		496.25	153.41	14.41	8	0.08	189.43	496.25	803.08
Be	norm		3.48	1.49	5.41	4	0.25	0.49	3.48	6.47
Ca	log		0.42	0.85	4.81	8	0.75	0.28	1.52	8.34
Ce	norm		98.42	27.25	4.02	7	0.75	43.92	98.42	152.91
Co	norm		23.48	8.66	10.41	7	0.15	6.17	23.48	40.79
Cr	log		4.54	0.38	6.70	6	0.40	44.04	93.99	200.62
Cu	norm		30.74	8.89	10.17	8	0.25	12.95	30.74	48.52
Fe	norm		4.93	1.39	11.76	8	0.15	2.14	4.93	7.71
Ga	norm	32	14.32	5.26	5.20	3	0.15	3.79	14.32	24.84
		68	28.67	2.67				23.32	28.67	34.02
K	norm		2.25	0.49	2.09	6	0.92	1.26	2.25	3.24
La	norm		47.78	13.27	4.39	7	0.75	21.25	47.78	74.31
Mg	norm		1.47	0.49	12.18	7	0.08	0.48	1.47	2.45
Mn	norm		0.12	0.03	7.00	6	0.40	0.06	0.12	0.18
Mo	log		−0.09	0.29	9.44	5	0.08	0.51	0.91	1.63
Na	norm	32	0.54	0.24	4.53	3	0.25	0.07	0.54	1.02
		68	1.60	0.39				0.82	1.60	2.37
Nb	log		2.76	0.52	7.37	8	0.45	5.56	15.78	44.76
Ni	norm		42.99	11.82	8.35	5	0.15	19.36	42.99	66.63
P	log		−2.10	0.34	7.21	6	0.30	0.06	0.12	0.24
Pb	log		3.37	0.39	11.37	6	0.08	13.30	28.96	63.07
Rb	norm		77.96	28.47	3.74	7	0.85	21.02	77.96	134.91
Sc	norm		16.43	4.09	12.67	12	0.40	8.24	16.43	24.61
Sn	norm		3.30	1.27	32.31	21	0.08	0.75	3.30	5.84
V	norm		147.12	38.84	6.83	8	0.60	69.44	147.12	224.79
Y	log		3.54	0.44	11.60	6	0.08	14.19	34.54	84.09
Zn	norm		92.79	25.97	8.21	5	0.40	40.84	92.79	144.74
Zr	norm		238.46	90.55	0.22	1	0.85	57.36	238.46	419.57
Carbonates										
Ag	log		−2.51	0.61	16.77	14	0.25	0.02	0.08	0.27
Al	norm		6.95	2.29	19.84	12	0.40	2.36	6.95	11.54
Ba	log		5.73	0.48	9.95	8	0.25	116.96	306.56	803.52
Be	norm		2.65	1.15	2.80	1	0.08	0.35	2.65	4.95
Ca	log	33	1.48	0.45	15.11	8	0.08	1.78	4.40	10.88
		67	2.36	0.34				5.32	10.59	21.08
Ce	norm		86.64	16.24	13.63	12	0.40	54.15	86.64	119.12
Cr	log		3.80	0.48	20.12	12	0.08	17.19	44.50	115.24
Fe	log		0.83	0.47	14.89	11	0.15	0.90	2.29	5.84
Ga	norm		14.37	6.67	11.15	7		1.04	14.37	27.70
La	norm		37.58	17.31	7.34	10	0.60	2.97	37.58	72.20
Mg	log		0.49	0.69	13.15	12	0.40	0.41	1.63	6.52
Mn	log		−2.98	0.50	39.83	29	0.08	0.02	0.05	0.14
Mo	norm	28	0.57	0.07	8.05	7	0.40	0.42	0.57	0.71
		72	0.87	0.27				0.32	0.87	1.41
Na	log		−0.64	0.62	20.41	12	0.08	0.15	0.53	1.84

Table 4 (*continued*)

Element	Dist	%	Mean	sdv	Chi2	*df*	*p*	Min	Mean	Max
Carbonates										
Nb	norm	41	13.45	3.70	7.58	7	0.40	6.05	13.45	20.84
		59	29.40	7.63				14.13	29.40	44.67
Ni	norm	63	22.11	5.09	9.14	8	0.40	11.93	22.11	32.28
		37	37.84	7.50				22.84	37.84	52.83
P	log		− 2.44	0.25	15.05	10	0.15	0.05	0.09	0.15
Pb	log		2.96	0.47	33.32	25	0.15	7.54	19.26	49.18
Sn	log		0.62	0.76	8.72	9	0.40	0.40	1.85	8.49
Sr	log		5.01	0.32	13.93	12	0.30	78.21	149.55	285.95
Ti	log		− 1.20	0.50	9.21	11	0.60	0.11	0.30	0.82
V	norm		97.31	38.68	14.77	9	0.08	19.96	97.31	174.67
Y	log		3.38	0.38	4.16	10	0.92	13.75	29.37	62.77
All other lithotypes										
Be	norm		3.51	1.40	3.08	4	0.60	0.72	3.51	6.31
Ca	log		0.20	0.46	12.52	19	0.85	0.49	1.22	3.07
			1.68	0.57				1.71	5.37	16.81
Ce	norm		96.48	24.66	33.13	24	0.15	47.17	96.48	145.80
Co	log		2.81	0.43	27.87	22	0.15	7.11	16.66	39.06
Cr	norm		68.79	26.24	26.18	23	0.25	16.30	68.79	121.27
Fe	norm		3.84	1.42	15.28	25	0.92	1.01	3.84	6.67
K	log		0.78	0.32	28.90	22	0.15	1.15	2.19	4.14
Mg	log		0.27	0.47	18.61	23	0.75	0.51	1.31	3.36
Mo	log		− 0.18	0.39	65.86	50	0.08	0.38	0.84	1.84
Na	log	46	− 0.44	0.72	28.19	20	0.18	0.15	0.64	2.73
		54	0.01	0.37				0.48	1.01	2.09
P	log		− 2.26	0.31	19.23	23	0.60	0.06	0.10	0.19
Pb	log		3.19	0.42	35.99	33	0.40	10.43	24.40	57.07
Rb	norm		88.49	35.33	37.35	25	0.08	17.83	88.49	159.14
Sc	norm		13.52	4.60	17.75	18	0.40	4.32	13.52	22.73
Sn	log		1.12	0.42	50.63	40	0.15	1.32	3.07	7.14
Ti	log		− 0.65	0.52	23.84	25	0.60	0.18	0.52	1.48
Zn	log		4.37	0.46	31.24	20		31.36	78.78	197.93

Minimum (min) and maximum (max) values of the populations are calculated by a distance of more than two standard deviations from the arithmetic or lognormal mean value (mean). Elements, which cannot be described by parametrical distribution functions, are not included.

geochemical processes within the catchments' basins are taken into account.

Bimodal distribution functions model an antagonistic data structure which is related to the lithological composition of the catchment basins. The population with high Ca, Rb and Ag concentrations is controlled by the presence of carbonates (Fig. 4), whereas the population with low values is found in metasedimentary rocks. The same structure exists for the elements Cr, Cu, Fe, Mn and Nb, in which high values are related to metasediments and low values to carbonates (Fig. 4). The observation of one single population in the frequency distributions reflects the fact that the dispersion of these elements is not dependent on the geochemical contrast between carbonates and metasediments.

In the concept of Sinclair (1974, 1991), anomalies are characterized by a parametrical data distribution which overlaps with the background population. However, anomalous samples in the Graz Paleozoic do not form such distributions. As a general rule, they are represented by values which cannot be explained by the modeled distribution functions. As proposed by Sinclair (1974, 1991), a 2σ-approximation of the background population was used to define a threshold between anomalous and background samples. The normal or log-normal distribution form of the background population was confirmed by performing a

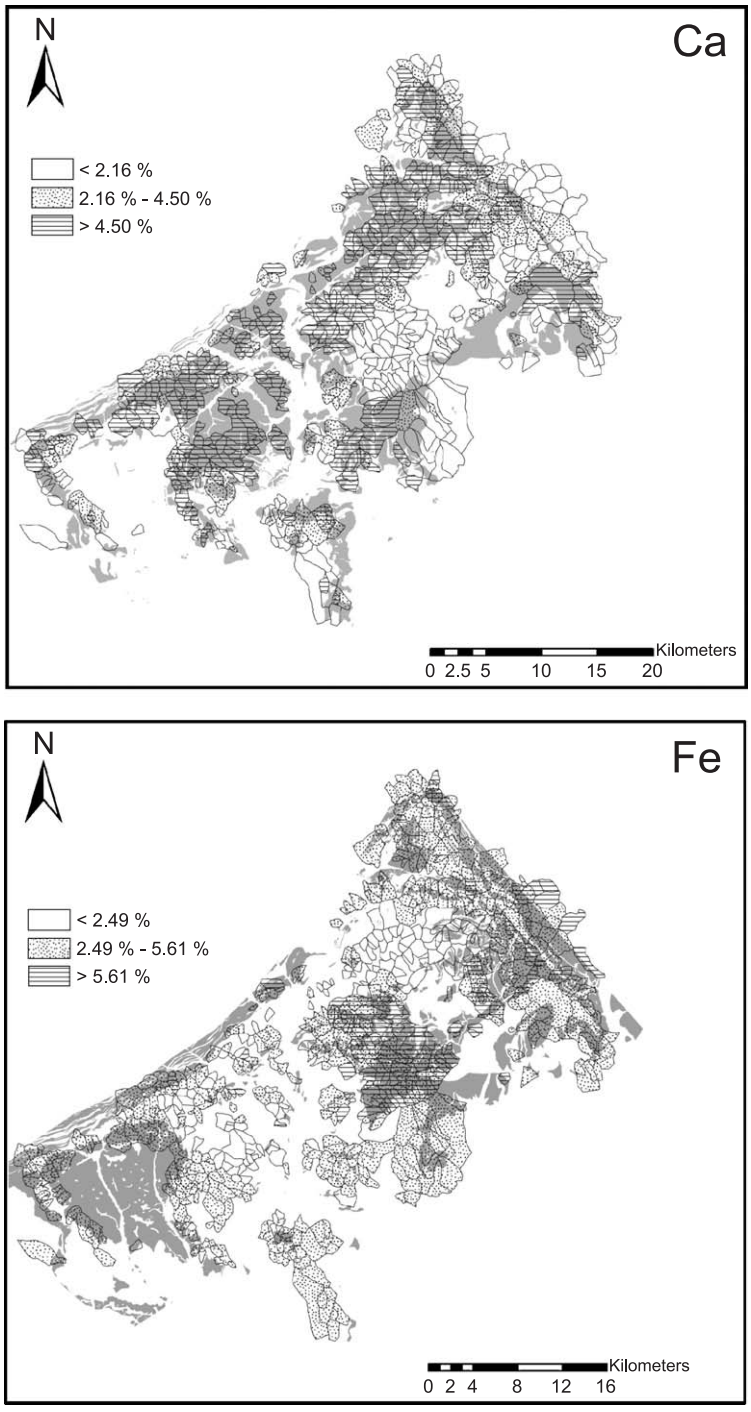

Fig. 4. Geochemical map of Ca and Fe in the Graz Paleozoic. Two overlapping populations are visualized by the lowest and highest class (see Table 2 and Fig. 2b). The intermediate class contains samples in the overlap region. Concentrations are assigned to the entire catchment area. The presence of carbonates in the Ca map and metasediments in the Fe map is indicated by the shaded background.

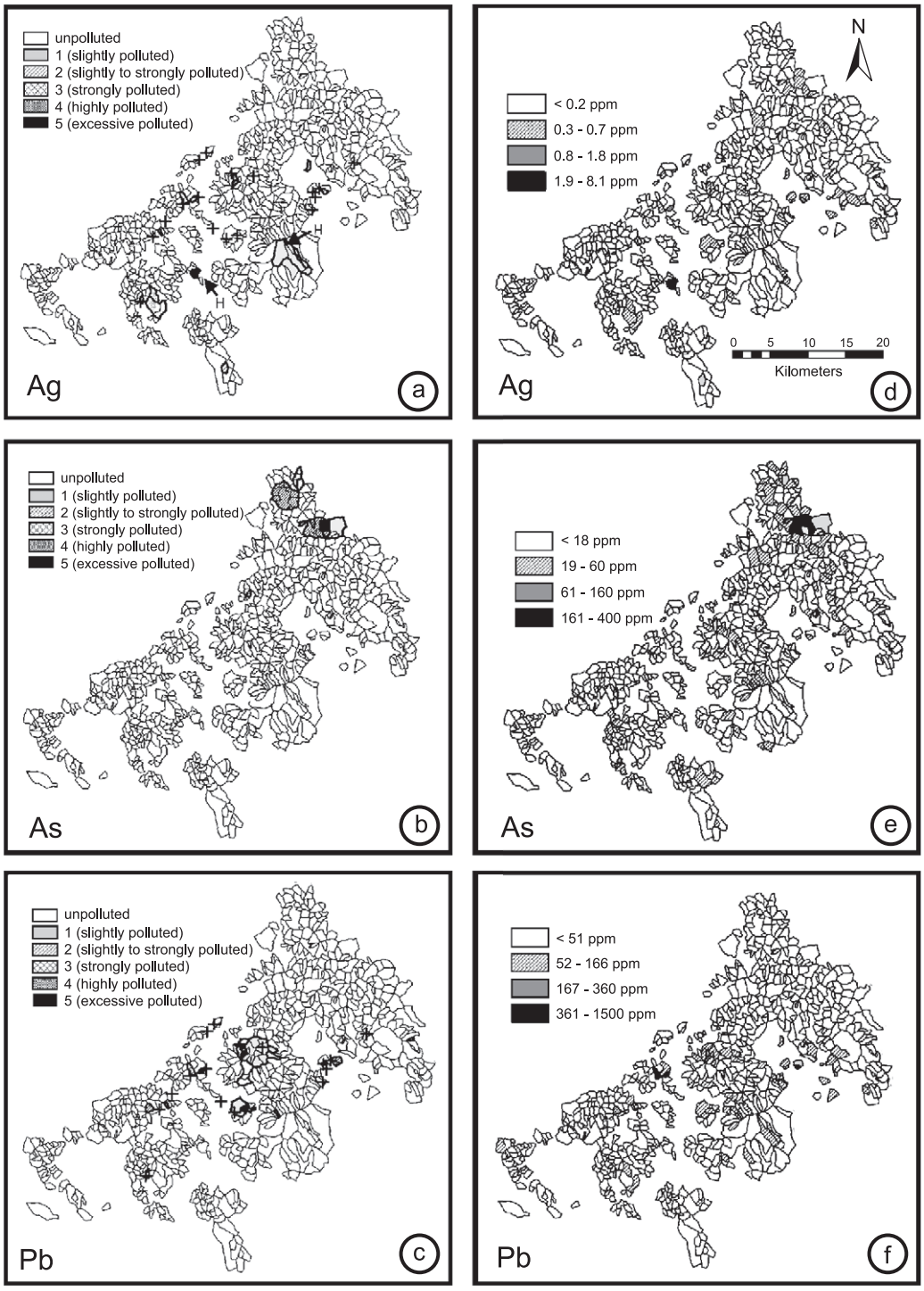
unpolluted
1 (slightly polluted)
2 (slightly to strongly polluted)
3 (strongly polluted)
4 (highly polluted)
5 (excessive polluted)
Ag
a
< 0.2 ppm
0.3 - 0.7 ppm
0.8 - 1.8 ppm
1.9 - 8.1 ppm
N
0 5 10 15 20
Kilometers
Ag
d
unpolluted
1 (slightly polluted)
2 (slightly to strongly polluted)
3 (strongly polluted)
4 (highly polluted)
5 (excessive polluted)
As
b
< 18 ppm
19 - 60 ppm
61 - 160 ppm
161 - 400 ppm
As
e
unpolluted
1 (slightly polluted)
2 (slightly to strongly polluted)
3 (strongly polluted)
4 (highly polluted)
5 (excessive polluted)
Pb
c
< 51 ppm
52 - 166 ppm
167 - 360 ppm
361 - 1500 ppm
Pb
f

Fig. 5.

chi-square test. Using the data of Tables 2–4, anomalies are expressed here by using the "Geoaccumulation index" (Igeo) proposed by Müller (1979) for the quantification of heavy metal accumulation in sediments. Igeo describes the relationship between the measured elemental concentration (Cn) and the upper limit of the background concentration (Bn) as:

$$\mathrm{Igeo} = \log2(\mathrm{Cn}/1.5\mathrm{Bn}).$$

The calculated indices are classified into seven enrichment classes ranging from class 0 (unpolluted) to class 5 (excessively polluted) and are assigned to the corresponding catchment areas (Fig. 5a–c). The mapped Geoaccumulation indices identify pathfinder elements for mineralisations and environmental pollutions. Environmental contaminations are detected by silver anomalies in the catchment areas of two hospitals (Fig. 5a). Arsenic is enriched in the area of arsenopyrite–gold mineralisations (Fig. 5b). Lead–zinc mineralisations are traced by higher Geoaccumulation indices for the element lead (Fig. 5c). Hence, the mapped Geoaccumulation indices show a high degree of spatial correlation between geochemical contaminations and mapped anomalies.

In Fig. 5, the resulting maps are compared to conventional geochemical maps. Geostatistical interpolation assumes a homogeneity of the underlying random process. However, in a complex geological setting, the heterogeneous lithological composition within the catchment area of the samples prevents the acceptance of this assumption (Rantitsch, 2001). As a second serious problem, the measured concentrations do not vary continuously, but have values within a fixed set of zones, given by the catchment areas. Therefore, the data values which are classified by a natural break method into four groups are assigned here to the entire catchment area of a sampling point (Fig. 5d–f). The comparison demonstrates that almost all Geoaccumulation index anomalies are mirrored by the concentration maps (Fig. 5). However, the measured elemental concentration of a sample value does not correspond with the rank of the enrichment factor. This discrepancy arises from the explicit consideration of the geochemical background concentration in the mapped Geoaccumulation indices, which is not visualized in concentration maps. Hence, when a measured concentration is evaluated with respect to a contamination, the view of a user is focused towards potential contaminations, not towards a lithologically induced concentration maximum. In addition, the ranking of the elemental enrichment evaluates the environmental impact of a contamination, which is hidden behind the data visualized in conventional geochemical maps.

Some elements show low ranked Geoaccumulation indices which cannot be attributed exactly to the site of a mineralisation or to the presence of a specific lithology. This observation must be explained by a different geochemical mobility, by analytically errors, by a different topographic setting which influences short-range hillslope processes (weathering, slope wash, mass wasting and soil creep), or by the fact that an anomaly near the sampling site will give a larger response than one distant from the sampling site (Moon, 1999).

It is suggested that multivariate statistical techniques cannot be used to study polypopulational geochemical data (Reimann and Filzmoser, 2000; Reimann et al., 2002). Weber and Davis (1990) performed a PCA by using the same database. Comparing the contour maps of the components which predict the locations of Pb–Zn and As mineralisations with the results of this study, it is obvious that both approaches give generally similar results. However, it is obvious that outlier severely influence the results of the PCA. This effect is seen by the example of the silver contamination (Geoaccumulation index of 5) in Fig. 5a which is not related to a Pb–Zn mineralisation. Although, all other elements of this site show "normal" concentrations, this single outlier results in a broad geochemical anomaly in a map of the multivariate mineralisation component (Fig. 6 in Weber and Davis, 1990). In contrast, the approach of this study does not detect a significant spatial correlation be-

Fig. 5. Maps (same area as in Fig. 4) of the Geoaccumulation index for Ag (a), As (b) and Pb (c) in the Graz Paleozoic including the locations of Pb–Zn (crosses) and Au–As (full square) mineralisations (Weber, 1997). The location of two hospitals (H) are shown in the Ag map. In alternative maps (d–f), the data values are classified by a natural break method into four groups and are assigned to the entire catchment area of a sampling point.

tween high Ag concentrations and the presence of Pb–Zn mineral deposits. Therefore, a misinterpretation of the anomaly is avoided.

6. Conclusions

In a geologically complex area, the variables of a regional geochemical data set can be described by parametrical distribution functions if the effects of downstream dilution and lithological background are taken into account. The results of this study indicate the catchment area and the lithological composition of the catchments as important factors which control the frequency distribution of large geochemical or environmental databases.

An inhomogeneous bedrock geology prevents the application of spatial statistics in the detection of geochemical anomalies. This problem can be resolved by the decomposition of frequency distribution into their components. This technique offers a simple technique to detect anomalous samples which can be explained by analytical errors, environmental contaminations or mineralisations.

Acknowledgements

The Geological Survey of Austria is acknowledged for providing the geochemical database. I am indebted to Ch. Li and an anonymous journal reviewer for their careful reviews on an earlier version of the manuscript.

References

Bölviken, B., Bogen, J., Demetriades, A., De Vos, W., Ebbing, J., Hindel, R., Langedal, M., Locutura, J., O'Connor, P., Ottesen, R.T., Pulkkinen, E., Salminen, R., Schermann, O., Swennen, R., Van der Sluys, J., Volden, T., 1996. Regional geochemical mapping of Western Europe towards the year 2000. J. Geochem. Explor. 56, 141–166.

Clark, I., 1977. ROKE a computer program for non-linear least-square decomposition of mixtures of distributions. Comput. Geosci. 3, 245–256.

Darnley, A.G., 1995. International geochemical mapping—a review. J. Geochem. Explor. 55, 5–10.

Hawkes, H.E., 1976. The downstream dilution of stream sediment anomalies. J. Geochem. Explor. 6, 345–358.

Limpert, E., Stahel, W.A., Abbt, M., 2001. Log-normal distributions across the sciences: keys and clues. BioScience 341, 341–352.

Matschullat, J., Ottenstein, R., Reimann, C., 2000. Geochemical background—can we calculate it? Environ. Geol. 39, 990–1000.

Moon, C.J., 1999. Towards a quantitative model of downstream dilution of point source geochemical anomalies. J. Geochem. Explor. 65, 111–132.

Müller, G., 1979. Schwermetalle in den Sedimenten des Rheines-Veränderungen seit 1971. Umschau 79, 778–785.

Plant, J., Smith, D., Smith, B., Williams, L., 2000. Environmental geochemistry at the global scale. J. Geol. Soc. (Lond.) 157, 837–849.

Rantitsch, G., 2000. Application of fuzzy clusters to quantify lithological background concentrations in stream-sediment geochemistry. J. Geochem. Explor. 71, 73–82.

Rantitsch, G., 2001. The fractal properties of geochemical landscapes as an indicator of weathering and transport processes within the Eastern Alps. J. Geochem. Explor. 73, 27–42.

Reimann, C., Filzmoser, P., 2000. Normal and lognormal data distribution in geochemistry: death of a myth. Consequences for the statistical treatment of geochemical and environmental data. Environ. Geol. 39, 1001–1014.

Reimann, C., Filzmoser, P., Garrett, R.G., 2002. Factor analysis applied to regional geochemical data: problems and possibilities. Appl. Geochem. 17, 185–206.

Sinclair, A.J., 1974. Selection of threshold values in geochemical data using probability graphs. J. Geochem. Explor. 3, 129–149.

Sinclair, A.J., 1991. A fundamental approach to threshold estimation in exploration geochemistry: probability plots revisited. J. Geochem. Explor. 41, 1–22.

Thalmann, F., Schermann, O., Schroll, E., Hausberger, G., 1989. Geochemischer Atlas der Republik Österreich 1: 1,000.000. Textteil. Geologische Bundesanstalt, Wien.

Weber, L. (Ed.), 1997. Handbuch der Lagerstätten der Erze, Industrieminerale und Energierohstoffe Österreichs. Arch. Lagerstättenforsch. Geol. Bundesanst. A, vol. 19. 607 pp.

Weber, L., Davis, J.C., 1990. Multivariate statistical analysis of stream-sediment geochemistry in the Grazer Paläozoikum, Austria. Mineral Deposita 25, 213–220.